Volume 16 No. 1
January 2024
ISSN : 2085 – 1669
e-ISSN : 2460 – 0288
Website : jurnal.umj.ac.id/index.php/jurtek
Email : jurnalteknologi@umj.ac.id

Jurnal Teknologi
UNIVERSITAS MUHAMMADIYAH JAKARTA

Prediction of Onset Temperature in Standing Wave Thermoacoustic Engine with Mesh Screen Stack

Prastowo Murti[1,*], Wijayanti Dwi Astuti[2], Ikhsan Setiawan[3], Fakih Irsyadi[2], Imroatul Hudati[2]
[1] *Department of Mechanical & Industrial Engineering, Faculty of Engineering, Universitas Gadjah Mada, Jl. Grafika No. 2, Yogyakarta 55281, Indonesia.*
[2] *Department of Electrical Engineering & Informatics, Vocational College, Universitas Gadjah Mada, Jl. Yacaranda, Sekip Unit IV, Yogyakarta. 55281, Indonesia.*
[3]*Departemen of Physics, Faculty of Mathematics and Natural Sciences, Universitas Gadjah Mada, Sekip Utara, Yogyakarta 55281, Indonesia*

*Corresponding author: prastowomurti@ugm.ac.id

Jurnal Teknologi use only:
Received 30 March 2023; Revised 22 September 2023; Accepted 26 September 2023

ABSTRACT

A thermoacoustic engine is a engine that converts thermal energy into acoustic energy, which can be used to generate electricity or cooling. This engine is attractive because it consists only of a stack, heat exchangers, and a resonator. The stack serves as the primary component for the energy conversion process and consists of porous materials like an array of stainless steel mesh screens. To generate the acoustic energy, a minimum temperature difference is necessary between the two sides of the stack, called the onset temperature difference. However, the calculation for prediction of onset temperature on the stack made of mesh screen has not been addressed. Therefore, the objective of this paper is to propose a method that can be used to estimate the onset temperature difference in standing wave thermoacoustic engine with stacks made of mesh screen arrays. The onset temperature difference is predicted numerically using linear stability theory and matrix transfer methods. Experimental verification is carried out by using standing wave thermoacoustic engine from pervious study. The results showed that the lowest onset temperature difference (T_H - T_C = 140ºC) is obtained when r_h = 0.497 mm. Furthermore, the numerical and experimental onset temperature difference comparisons show a qualitative agreement, allowing the onset temperature prediction method to be used in designing standing wave thermoacoustic engines with stacks made of mesh screens.

Keywords: onset temperature, thermoacoustic engine, standing wave, stack mesh screen.

Introduction

A thermoacoustic engine is a device that transforms heat energy into acoustic energy, which can be harnessed either for electricity generation [1] or for powering a cooling system [2]. Generally, thermoacoustic engines are categorized into two types based on the phase difference between pressure oscillations and the velocity of the working gas within the stack: standing wave thermoacoustic engines with straight pipe resonators (depicted in Figure 1(a)) and traveling wave engines with circular pipe resonators (shown in Figure 1(b)). Researchers have shown interest in these engines due to their eco-friendly nature, absence of greenhouse gas emissions, straightforward design, and the ability to utilize waste heat as an energy source, placing them in the category of external combustion engines [3].

DOI: https://dx.doi.org/10.24853/jurtek.16.1.27-32

ISSN : 2085 – 1669
e-ISSN : 2460 – 0288

One approach to reduce the onset temperature is by optimizing the hydraulic radius of the stack. The hydraulic radius is a critical parameter used to determine the size of the pores in the stack. The correct pore size is essential for achieving a low onset temperature by facilitating efficient interaction between the working gas and the stack. Abduljalil explored various stack materials and found that a mesh screen arrangement resulted in a lower onset temperature compared to other materials [4]. Hariharan investigated how the hydraulic radius of parallel plate stacks affects the onset temperature difference [5]. Both experimental and simulation results indicated that the hydraulic radius significantly influences thermoacoustic engine performance. Sakaguchi examined the effects of different hydraulic radii of mesh screen stacks and stack locations on the onset temperature variation [6]. The observations revealed that there are optimum values for both the hydraulic radius of the mesh screen stack and the stack's location for each thermoacoustic engine.

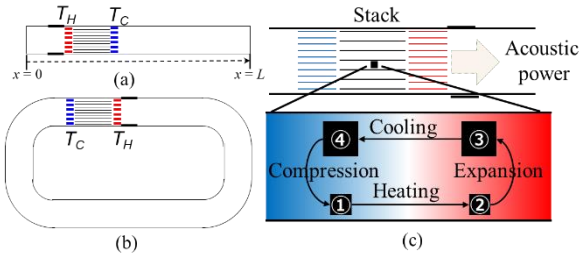

Figure 1. Schematic diagram of standing wave (a) and traveling wave (b) thermoacoustic engine. A Thermodynamic cycle occurs in the stack (c).

Based on the references mentioned above, it is evident that using a stack made of a mesh screen arrangement offers advantages over other materials, including ease of availability, cost-effectiveness, and high thermal conductivity. However, determining the optimal hydraulic radius can be a time-consuming and costly trial-and-error process. Ueda developed a method to predict the onset temperature for both standing wave thermoacoustic engines (Figure 1(a)) and traveling-wave engines (Figure 1(b)) [7]. Similarly, Hyodo proposed a method for predicting the onset temperature in combined loop and straight-tube thermoacoustic engines [8]. However, their calculations were based on stacks with cylindrical or parallel plate pores, while stacks with mesh screen pores, which exhibit random characteristics, remained unexplored. Consequently, there is a need for a method to predict the onset temperature of thermoacoustic engines that utilize stacks made of mesh screens.

The aim of this study is to develop a method for predicting the onset temperature of a standing wave thermoacoustic engine with a mesh screen stack. The calculation of the onset temperature relies on the general thermoacoustic equation. A standing wave thermoacoustic engine was constructed to validate the calculation results. The comparison of results indicates a qualitative agreement between the calculated and experimental onset temperatures, demonstrating the potential of this method for use in the design of standing wave thermoacoustic engines having mesh screen stack.

Thermoacoustic Engine Model

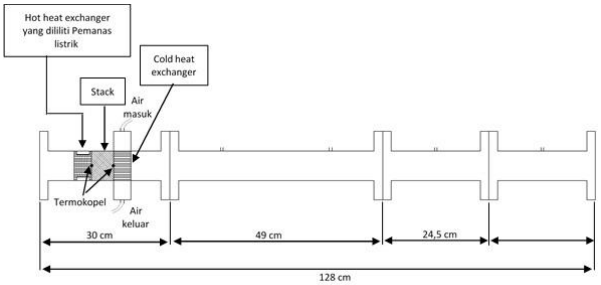

Figure 2. Schematic diagram of standing wave thermoacoustic by ref. [9] .

Tabel 1. Calculation of r_h *stack mesh screen*

Mesh number (/inch)	r_h (mm)
8	0,903
10	0,713
12	0,583
14	0,497
18	0,381

In this study, we used standing wave thermoacoustic engine having mesh screen stack from previous study [9]. Figure 2 shows a schematic diagram of standing wave thermoacoustic engine. The resonator length was 128 cm with 6.8 cm inner diameter. The hot heat exchanger was made of copper

Jurnal Teknologi 16 (1) pp 27-32 © 2024

cylinders with a diameter of 6.8 cm, a length of 3 cm, and 40 axial holes with a diameter of 2.5 mm. The cold heat exchanger was also made of copper cylinders with a diameter of 6.8 cm, a length of 4 cm, and axial holes with a diameter of 2 mm. The stack was made up of layers of wire mesh screens with mesh numbers #8, #10, #12, #14, and #18, with stack lengths ranging from 3 to 6 cm. Table 1 provides calculations for the hydraulic radius of the mesh screen stack material. The working gas was air at atmospheric pressure and temperature.

Calculation Method

To predict the onset temperature of a thermoacoustic engine, the general equation used is the acoustic approximation, which is based on Rott's approach to the hydrodynamic equations of energy, momentum, and continuity [10]. These equations assume that the acoustic variables obtained represent mean values, and it accounts for slight changes in the angular frequency $\omega = 2\pi f$ of the system. Consequently, the equation mentioned above is transformed into a set of coupled differential equations describing the complex pressure p_1, and the complex velocity v_1, of the gas

$$\frac{dp_1}{dx} = -i\omega \frac{\rho_m}{A} \frac{1}{1-\chi_v} v_1, \tag{1}$$

$$\frac{dv_1}{dx} = -i\omega \frac{A\left[1+(\gamma-1)\chi_\alpha\right]}{\gamma P_m} p_1 + \frac{\chi_\alpha - \chi_v}{(1-\chi_v)(1-Pr)} \frac{1}{T_m} \frac{dT_m}{dx} \tag{2}$$

where T_m, ρ_m, P_m, γ, and Pr denote temperature, desnity, pressure, specific heat ratio, dan *Prandtl number* of working gas. A denotes cross-sectional area of tube. χ_j is thermoacoustic function as

$$\chi_j = \frac{2J_1\left[(\mathrm{i}-1)\frac{r_0}{\delta_j}\right]}{(\mathrm{i}-1)\frac{r_0}{\delta_j} J_0\left[(\mathrm{i}-1)\frac{r_0}{\delta_j}\right]}, \tag{3}$$

$$\delta_j = \sqrt{2j/\omega} \tag{4}$$

where $j = \alpha$ (gas thermal diffusivity) atau v (gas kinematic viscosity) and r_0 is radius of tube.

When the right-hand side of equations (1) and (2) is considered constant within a channel segment of length L, these equations can be solved analytically and expressed as such (Hyodo et al., 2017)

$$\begin{pmatrix} p(x+\Delta x) \\ v(x+\Delta x) \end{pmatrix} = M_R \begin{pmatrix} p(x) \\ v(x) \end{pmatrix}, \tag{5}$$

where M_R denotes transfer matrix with

$$M_R = e^{\frac{GL}{2}} \begin{pmatrix} -\frac{G}{\tau}\sinh(\lambda)+\cosh(\lambda) & \frac{2Z}{\tau}\sinh(\lambda) \\ \frac{2Y}{\tau}\sinh(\lambda) & \frac{G}{\tau}\sinh(\lambda)+\cosh(\lambda) \end{pmatrix}, \tag{6}$$

and

$$G = \frac{\chi_\alpha - \chi_v}{(1-\chi_v)(1-Pr)} \frac{1}{T_m} \frac{dT_m}{dx} \tag{7}$$

$$Y = i\omega \frac{A\left[1+(\gamma-1)\chi_\alpha\right]}{\gamma P_m} \tag{8}$$

$$Z = -i\omega \frac{\rho_m}{A} \frac{1}{1-\chi_v} \tag{9}$$

$$\tau = \sqrt{G^2 + 4YZ} \tag{10}$$

$$\lambda = \tau L / 2. \tag{11}$$

The transfer matrix for the stack M_{stk}, and the thermal buffer tube M_{tbt}, is the same as equation (6). Meanwhile, the transfer matrices for the resonator M_t, and the heat exchangers (M_{HE} for the hot heat exchanger and M_{CE} for the cold heat exchanger) are also the same as in equation (6), but with $G=0$ since there is no temperature change occurring along the resonator and heat exchangers. The channel radius in the transfer matrix for the stack M_{stk} is calculated using the hydraulic radius equation r_h for randomly porous materials (wire mesh screen) as [11]

$$r_h = D_{wire} \frac{\phi}{4(1-\phi)}, \tag{12}$$

where D_{wire} is diameter of wire mesh screen and ϕ is porosity of mesh screen calculated by

$$\phi = 1 - \frac{\pi n D_{wire}}{4} \tag{13}$$

where n is wire mesh screen number.

According to Fig. 1(a), a standing wave thermoacoustic engine consists of a resonator, heat exchangers, stack, and thermal buffer tube. Thus, the overall transfer matrix Mall is

ISSN : 2085 – 1669
e-ISSN : 2460 – 0288

obtained by multiplying several segments together

$$M_{all} = M_t M_{CE} M_{stk} M_{HE} M_{tbt} M_t . \quad (14)$$

It is important to note that these calculations neglect nonlinear effects and minor losses to simplify the computations [7]. When the complex amplitudes of acoustic pressure and volumetric velocity of the gas at the location $x = 0$ (see Figure 1(a)) are denoted as p_0 and v_0, then the pressure and volumetric velocity at the end of the resonator pipe are p_L and v_L, respectively. Therefore, equation (5) can be written as follows

$$\begin{pmatrix} p_L \\ v_L \end{pmatrix} = M_{all} \begin{pmatrix} p_0 \\ v_0 \end{pmatrix} . \quad (15)$$

Since both ends of the resonator are closed, v_0 and v_L must be equal to zero, making equation (15) become

$$\begin{pmatrix} p_L \\ 0 \end{pmatrix} = M_{all} \begin{pmatrix} p_0 \\ 0 \end{pmatrix} . \quad (16)$$

p_0 dan p_L at Eq. (16) is non zeo if m_{21} is zero or

$$m_{21} = 0 , \quad (17)$$

where m_{21} is an element of M_{all}.

The onset temperature is obtained by solving a solution from the left-hand side of Eq. (17) as a function of the angular frequency $y(\omega)$ when provided with values for the hydraulic radius of the stack r_h and the hot heat exchanger temperature T_H. The Secant method is employed to find the solution for $y(\omega) = 0$ by providing an initial value ω_0 or ω_1 that approaches the fundamental angular frequency of the system. The calculation proceeds until the convergence condition is met, where ω_n and ω_{n+1} are

$$\omega_{n+1} = \omega_n - \frac{\omega_n - \omega_{n-1}}{y(\omega_n) - y(\omega_n)} y(\omega_n). \quad (18)$$

The solution for ω is a complex number, where the real part represents the fluctuation in the angular frequency of the thermoacoustic engine, and the imaginary part reflects the system's stability. When the imaginary part of ω is positive, the system is in a stable state, meaning there are no spontaneous oscillations of the working gas. When ω becomes a real number, the system is in a neutrally stable state. On the other hand, when the imaginary part of ω is negative, the system is in an unstable state, indicating spontaneous oscillations of the working gas within the system [8]. The temperature difference between the hot heat exchanger T_H and the cold heat exchanger T_C under unstable conditions is referred to as the onset temperature difference.

Results and Discussions

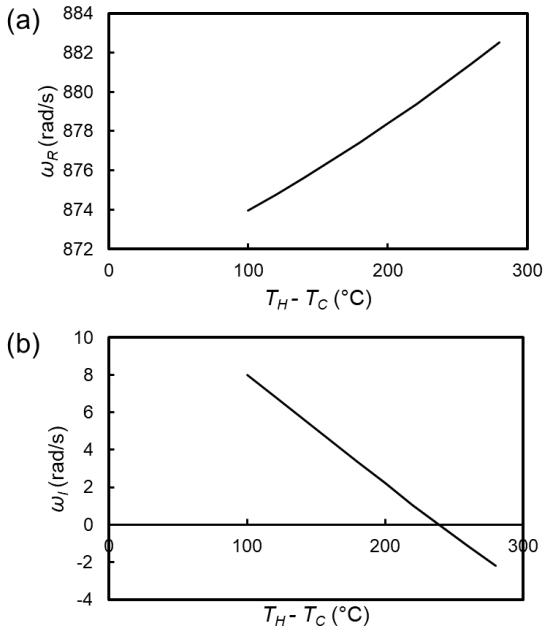

Figure 3. Influence of temperature difference (T_H-T_C) on real part ω_R (a) dan imaginary part ω_I (b) when stack wire mesh screen with r_h = 0.713 mm and length of 6 cm.

Figure 3(a) and 3(b), respectively, illustrate the influence of temperature difference on the real part ω_R and the imaginary part ω_I of the complex frequency of the system when the stack has r_h = 0.713 mm and a length of 6 cm. In Fig. 3(a), it can be observed that ω_R gradually increases with T_H-T_C. Meanwhile, in Fig. 3(b), ω_I slowly decreases from positive values to negative ones and crosses $\omega_I = 0$ when T_H-T_C = 240 ºC. The condition where $\omega_I = 0$ represents the moment just before spontaneous oscillations occur, known as the critical temperature. Therefore, the onset temperature (when oscillations occur) is determined in the calculations when $\omega_I > 0$ (negative).

Figure 4 shows the calculation and experimental results of the onset temperature difference concerning the hydraulic radius and the length of the mesh screen stack in the

Jurnal Teknologi 16 (1) pp 27-32 © 2024

standing wave thermoacoustic engine. It can be observed that a hydraulic radius of r_h = 0.497 – 0.583 mm yields the lowest onset temperature difference compared to others for all stack lengths. Additionally, it's evident that increasing the stack length leads to an increase in the onset temperature.

When the r_h value is large, the working gas requires a significant amount of heat to oscillate and transfer heat to the stack walls due to the substantial distance between them, resulting in a high onset temperature. Similarly, when r_h is small, the working gas faces difficulties in oscillating due to viscous losses, which cause an increased heat requirement, leading to a higher onset temperature [11]. Meanwhile, the stack length affects the onset temperature because it determines the amount of heat required to reach the minimum oscillation temperature.

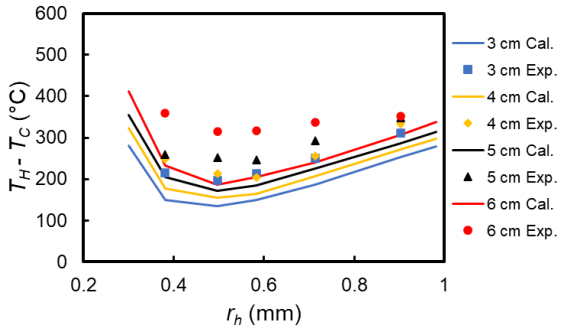

Figure 4. Hydraulic radius r_h as a function of temperature difference T_H-T_C. Lines denote calculation results, whereas symbols denote experimental results by ref [9].

From Fig. 4, it can also be concluded that the difference in onset temperature between the calculation and the experiment shows qualitative agreement. The discrepancy between them is attributed to heat loss and viscous losses that occur during the experimental process, which are not considered in the calculations. We consider by Adding thermal insulation around the stack and heat exchangers will result in a reduction of the discrepancy. Therefore, it can be concluded that the proposed calculation method can be used to predict the onset temperature when one intends to construct a standing wave thermoacoustic engine, saving both time and costs.

Conclusions

This study presents a numerical method to predict the onset temperature difference in the standing wave thermoacoustic engine using a stainless steel mesh screen stack. Verification of the calculations was carried out against previous result. The results indicate that the onset temperature prediction qualitatively aligns with experimental results. It is expected that the findings of this study can reduce the costs and time required in the design process of standing wave thermoacoustic engines.

Acknowledgment

Prastowo Murti would like to thank Professor Tetsushi Biwa from Tohoku University for providing an opportunity to learn about stability limit analysis.

Funding

This research was funded by the Community Research Grant of the Vocational College Number: 103/UN1/SV/PPM/PT/2023.

Author Contributions

Prastowo Murti, Wijayanti Dwi Astuti, Fakih Irsyadi, Imroatul Hudati: Methodology, Software, Data curation, Writing – original draft. Ikhsan Setiawan: Writing – review & editing. Prastowo Murti, Wijayanti Dwi Astuti: Software, Validation, Supervision.

Conflicts of Interest

The authors declare no conflict of interest.

References

[1] Backhaus, S., Tward, E. and Petach, M., Traveling-Wave Thermoacoustic Electric Generator, *Applied Physics Letters*, vol. **85**, no. 6, 2004. DOI: 10.1063/1.1781739

[2] Murti, P., Setiawan, I., Fadly, M. and Murtyas, S. D., Pengaruh Jejari Hidrolik Regenerator Dan Frekuensi Gelombang Bunyi Terhadap Kinerja Pompa Kalor Termoakustik Gelombang …, *Jurnal Teknologi*, vol. **10**, no. 2, 2018.

[3] Setiawan, I., Murti, P., Achmadin, W. N. and Nohtomi, M., Pembuatan Dan Pengujian Prime Mover Termoakustik Tipe Gelombang Tegak, *Proceeding*

ISSN : 2085 – 1669
e-ISSN : 2460 – 0288

Seminar Nasional Tahunan Teknik Mesin XIV (SNTTM XIV), no. Snttm Xiv, 2015.

[4] Abduljalil, A. S., Yu, Z. and Jaworski, A. J., Selection and Experimental Evaluation of Low-Cost Porous Materials for Regenerator Applications in Thermoacoustic Engines, *Materials and Design*, vol. **32**, no. 1, 2011. DOI: 10.1016/j.matdes.2010.06.012

[5] Hariharan, N. M., Sivashanmugam, P. and Kasthurirengan, S., Influence of Stack Geometry and Resonator Length on the Performance of Thermoacoustic Engine, *Applied Acoustics*, vol. **73**, no. 10, 2012. DOI: 10.1016/j.apacoust.2012.05.003

[6] Sakaguchi, A., Sakamoto, S. I., Tsuji, Y. and Watanabe, Y., Energy Conversion from Sound to Heat Using Lamination Mesh on the Thermoacoustic System, *Japanese Journal of Applied Physics*, vol. **48**, no. 7 PART 2, 2009. DOI: 10.1143/JJAP.48.07GM13

[7] Ueda, Y. and Kato, C., Stability Analysis of Thermally Induced Spontaneous Gas Oscillations in Straight and Looped Tubes, *The Journal of the Acoustical Society of America*, vol. **124**, no. 2, 2008. DOI: 10.1121/1.2939134

[8] Hyodo, H., Muraoka, K. and Biwa, T., Stability Analysis of Thermoacoustic Gas Oscillations through Temperature Ratio Dependence of the Complex Frequency, *Journal of the Physical Society of Japan*, vol. **86**, no. 10, 2017. DOI: 10.7566/JPSJ.86.104401

[9] Prastowo Murti, Adhika Widyaparaga, Ikhsan Setiawan, Bambang Agung Setyo Utomo and Makoto Nohtomi, Pengaruh Jejari Hidrolik Stack Terhadap Beda Suhu Onset Pada Prime Mover Termoakustik Gelombang Berdiri, *Spektra: Jurnal Fisika Dan Aplikasinya*, vol. **16**, no. 2, pp. 36–40, 2015.

[10] Rott, N., Thermally Driven Acoustic Oscillations. Part II: Stability Limit for Helium, *Zeitschrift Für Angewandte Mathematik Und Physik ZAMP*, vol. **24**, no. 1, 1973. DOI: 10.1007/BF01593998

[11] Swift, G. W. and Garrett, S. L., Thermoacoustics: A Unifying Perspective for Some Engines and Refrigerators , *The Journal of the Acoustical Society of America*, vol. **113**, no. 5, 2003. DOI: 10.1121/1.1561492